DTI-based Segmentation and Quantification of Human Brain Lateral Ventricular CSF Volumetry and Mean Diffusivity: Validation, Age, Gender effects and Biophysical Implications

Khader M. Hasan, PhD[1,CA], **F. Gerard Moeller**[2], and **Ponnada A. Narayana, PhD**[1]

[1]Medical School, Departments of Diagnostic and Interventional Imaging, The University of Texas Health Science Center, Houston, Texas, USA

[2]Department of Psychiatry, Pharmacology and Toxicology, Virginia Commonwealth University School of Medicine

Abstract

The human brain lateral ventricular (LV) cerebrospinal fluid (CSF) volume has been used as a neuroimaging marker of brain changes in health and disease. The LV CSF diffusivity may offer a useful quality assurance measure and become a potential noninvasive marker of deep brain temperature. In this work we sought to validate a method for human brain lateral ventricular (LV) cerebrospinal fluid (CSF) using diffusion tensor imaging (DTI) contrast to provide LV volume and corresponding DTI metrics. We compared LV volume obtained using DTI with that obtained using validated segmentations of the LV on T1-weighted data. DTI and T1-weighted data were acquired at 3 T on 49 healthy males and 56 age-matched females aged 18–59 years. We showed histogram distributions of LV DTI metrics to establish quality assurance measures. We also analyzed the age and gender effects of LV volume and diffusivity. LV volumes estimated using both T1-weighted and DTI correlated strongly in males and females (ICC=0.99; median Dice index ~80%). The LV-to-intracranial volume percentage increased significantly with age only in males, using the DTI-based approach (r=0.39; p=0.005). LV CSF Mean diffusivity was greater in males than females ((~1.2%; p=0.03). Mean diffusivity of lateral ventricular CSF decreased significantly with age in healthy adults (r=−0.30; p=0.02). Our results highlight the importance of age and gender-based analyses and the potential of LV diffusivity measures as a quantitative marker.

CACorresponding Author: Khader M. Hasan, Ph.D., Associate Professor of Diagnostic and Interventional Imaging Department of Diagnostic and Interventional Imaging University of Texas Health Science Center at Houston 6431 Fannin Street, MSB 2.100 Houston, Texas 77030, Tel: Office (713) 500-7690 Fax: (713) 500-7684, Khader.M.Hasan@uth.tmc.edu.

Publisher's Disclaimer: This is a PDF file of an unedited manuscript that has been accepted for publication. As a service to our customers we are providing this early version of the manuscript. The manuscript will undergo copyediting, typesetting, and review of the resulting proof before it is published in its final citable form. Please note that during the production process errors may be discovered which could affect the content, and all legal disclaimers that apply to the journal pertain.

---

1. Introduction

Due to its close interplay with the vasculature, cerebrospinal fluid (CSF) plays a role in regulating the intracranial pressure and biochemical activity [1]. The whole brain, sulcal, and ventricular CSF volumes have been used to follow normal brain development and natural aging across the lifespan [2, 3]. In particular, the lateral ventricles (LV), owing to the relative ease of their identification and segmentation using manual and automatic methods utilizing magnetic resonance imaging (MRI) contrast, have been shown to increase in volume with age in healthy adults [3, 4, 5]. Ventricular volume enlargement has been used as a surrogate marker in a host of pathologies [6, 7, 8]. CSF chemical and metabolic contents serve as robust biomarkers of neural degeneration [9, 10]. In addition, LV-CSF diffusivity combined with diffusion vs. temperature measurements has been used recently to estimate core brain temperature [11, 12].

Cross-sectional and longitudinal studies reported an average rate of increase in the LV volume of 0.5 mL/year in young and middle-aged adults (18–60 years), while rate faster than ~ 1 mL/year may be expected in advanced aging [5]. The increase in LV volume with age was shown to be significantly slower in healthy females than in males [4, 13, 14] and hence the effect of age and gender on the CSF volumetry has to be examined in interpreting the CSF volume.

Several computational methods have been described to segment, and validate brain parenchyma and CSF volumetry [7, 8]. A recent work by Kempton et al. [8] presented a framework for testing LV segmentation from high resolution T1-weighted data using manual and three automated methods that included FreeSurfer (http://surfer.nmr.mgh.harvard.edu/fswiki), FSL-FIRST (http://fsl.fmrib.ox.ac.uk/fsl/fslwiki/FIRST) and SPM-ALVIN (https://sites.google.com/site/mrilateralventricle/). These authors concluded that the LV segmentation using T1-weighted data and FreeSurfer is most reliable for the application to healthy controls and patients with Alzheimer's disease [8].

A comprehensive analysis of normative LV volumetry, anisotropy and diffusivity using diffusion tensor imaging (DTI) measurements on healthy young and middle-aged males and females has not been described previously.

Due to continuous production of CSF by the choroid plexus, regional variability in concentration and temperature, the CSF diffusivity may not be spatially uniform over the entire LV. The LV CSF diffusivities may be overestimated due to flow and pulsatile motion or underestimated due to partial averaging with brain parenchyma especially at the edges of LV [12]. The availability of spatially-normalized maps and histogram distributions of the corresponding DTI metrics on healthy subjects would provide useful quantitative measures for clinical applications.

In this Report, we aimed to extend a previously described DTI-based segmentation [15] and DTI- and atlas-based parcellation [16] method to the CSF spaces, particularly in the LV. Following the recommendations by Kempton et al. [8], we validated the new DTI-based CSF segmentation by comparing the LV volumes obtained using the DTI data with those obtained with FreeSurfer pipeline applied to the T1-weighted data acquired from same subjects. We studied the spatial distribution of the lateral ventricular DTI metrics to provide baseline reference values for future applications. We also investigated the age dependence of LV volume and its CSF diffusivity in a cohort of age-matched healthy men and women to examine the sensitivity of the approach in capturing age and gender-based differences in LV macrostructural and microstructural attributes.

2. Subjects and Methods

2.1 Participant Demographics

This protocol was approved by our Institutional Review Board. Written informed consent was obtained from each participant prior to scanning. Based on the review of medical history and MRI by a board certified radiologist all participants were considered normal and healthy. The participants included 105 healthy adults with 49 males (age range = 18.7–57.6 years; mean age $\pm$ SD = 33.1 $\pm$ 10.5 years) and 56 females (age range = 19–56.9; mean age $\pm$ SD = 36.3 $\pm$ 10.5 years).

2.2 MRI Data Acquisition

We acquired whole-brain data on a Philips 3.0 T Intera scanner with a dual quasar gradient system with maximum gradient amplitude of 80 mT/m, maximum slew rate of 200 mT/m per millisecond, and an eight-channel SENSE compatible head coil (Philips Medical Systems, Best, Netherlands). All sequences were acquired without respiratory or cardiac gating.

2.2.1 Anatomical High Resolution T1w—The T1-weighted data were acquired using the 3D spoiled gradient-echo sequence (3D-SPGR) with a field-of-view (FOV) of 240×240 mm^2 and isotropic voxel size of 0.9375 mm, echo time (TE) = 3.7 ms, and repetition time (TR) = 8.1 ms. The total scan time was 6 minutes.

2.2.2 DTI Data Acquisition—The diffusion-weighted data were acquired using a single-shot spin echo diffusion sensitized echo-planar imaging (EPI) sequence with the balanced *Icosa21* encoding scheme which uses twenty-one diffusion gradient orientations (17), a diffusion sensitization of b = 1000 s.mm^{-2}, TR = 6.1 s, TE = 84 ms. EPI image distortion artifacts were reduced by using a SENSE acceleration factor or k-space under sampling of R of two. The slice thickness was 3 mm with 44 axial slices covering the whole-brain (foramen magnum to vertex), FOV = 240×240 mm^2, and an image matrix of 256×256 after k-space reconstruction (i.e. in-plane voxel size matched T1-weighted data). The number of non-diffusion weighted or b~0 magnitude image averages was 8; in addition, each encoding was repeated twice and magnitude-averaged to enhance the signal-to-noise ratio(17).

2.3. MRI Data Processing

The MRI data processing pipeline used in this work is described in more detail elsewhere [16, 18], and here we provide a brief description of the major processing steps.

2.3.1 Segmentation and Parcellation of T1-weighted Data—The T1-weighted brain data were automatically segmented into cortical, subcortical, and CSF compartments using FreeSurfer software library [19]. We used FreeSurfer (version 5.1; http:// surfer.nmr.mgh.harvard.edu/) in our work to validate the DTI-based ventricular volumes as it has been previously validated [9, 20] and applied on the healthy cohort used in this study as detailed elsewhere [18].

2.3.2 DTI-Processing—The non-diffusion (b0) volumes were averaged by the scanner and the output volume was masked using the brain extraction tool (BET, http:// www.fmrib.ox.ac.uk/fsl/bet2/index.html) which is incorporated in MRIcro (http:// www.cabiatl.com/mricro/mricro/mricro.html) and the mask was used to remove non-brain tissue from the DWI volumes. The DWI volumes were coregistered to the b0 image volume using the affine transformation. DWI volumes were then decoded and diagonalized to obtain the scalar and vector maps [21]. The scalar maps included the tensor eigenvalues which were used to compute mean diffusivities (MD). The intracranial volume (ICV) was obtained by summing the total GM (cerebral and cerebellar), WM and cerebrospinal CSF (ventricular and sulcal) volumes [15].

2.3.3 Lateral Ventricular Segmentation using DTI Tissue Contrast—The DTI scalar maps were used to facilitate regional tissue segmentation [15] and parcellation using SPM2 unified and multi-modal segmentation [22] implemented in SPM (http:// www.fil.ion.ucl.ac.uk/spm/) as detailed elsewhere [16]. In brief, the segmentation of CSF utilized the high contrast between brain parenchyma and CSF in the FA vs. mean diffusivity space (Figure 1A). The automatic identification of LV in native space utilized a binary mask of the LV in MNI space built from a large cohort of normal subjects [9; https:// sites.google.com/site/mrilateralventricle/]. The segmentation of the LV in the native space was achieved after applying the inverse spatial normalization parameters for each subject to the LV mask [9].

To assure reliability of the data, we applied the same transformations to the subcortical and cortical gray matter [23] and white matter [24] provided by the international consortium for brain mapping (ICBM; http://www.loni.ucla.edu/Atlases/) as described previously [16]. We also obtained global or whole brain CSF [2, 15] and masked out segmented ventricular CSF to obtain sulcal CSF [13]. Figure 1B shows a two-dimensional scatter plot of MD vs. FA [15, 25] for a host of structures that included neocortex, hippocampus, caudate, putamen, genu and splenium of corpus callosum (CC), posterior thalamic radiations (PTR), superior longitudinal fasciculus (SLF), in relation to the lateral ventricles.

2.3.4 Quantification of LV using DTI metrics and Data Quality Assurance—The DTI-based segmentation procedure provided a mask of the LV in each subject's native space that was used to estimate the volume by counting the number of voxels and multiplying by

the voxel volume. To compare and assess spatial overlap between the DTI-based and the T1w LV segmentations we realigned the b0 map unto the T1w volume using normalized mutual information and carried the transformation unto the LV mask using nearest neighbor interpolation. We then estimated the Dice overlap index which is defined as the percentage of spatial overlap volume between the DTI-based and T1w-based masks to the mean value of the two volumes [8, 19].

In addition, we estimated the LV corresponding DTI-derived metrics such as the diffusivities and fractional anisotropy on each subject. To assure the accuracy of the estimated DTI metrics of the LV and reduce contamination of LV with bordering brain tissue we eroded [26, 27] the LV mask at different erosion levels (i.e. level 0 = no erosion, level 1 = eroded ~1/3 of original volume, level 2 eroded ~ 1/2 of original mask volume, etc.). We also pooled the LV voxels on all 105 healthy subjects to examine closely the histogram distribution of the LV corresponding DTI metrics to help reject potential outliers [12] due to non-random motion (i.e. flow, pulsation).

To assure scanner stability during the ~ 4 years of data acquisition, we also acquired data using identical DTI protocol on spherical water phantom data. The water DTI phantom data were analyzed from a central region-of-interest to assure temporal stability using quality assurance measures described previously [28].

2.4. Statistical Analysis

Group comparisons (e.g. males vs. females) were conducted using unpaired t-tests. Comparisons between LV volume obtained with FreeSurfer-T1w and SPM-DTI were inspected using Bland-Altman bias analysis, linear regression scatter plots, paired t-tests, the intraclass correlation coefficient [29] and the Dice spatial overlap percentage as described above. Correlations of LV-to-ICV percentage with age were computed using the Pearson correlation coefficient and comparisons between slopes used the z-Fisher transform [30]. All computations and statistical analyses were conducted using MATLAB (The Mathworks Inc, Natick, MA, USA).

3. Results

The healthy men and women in our cohort did not differ in age (p = 0.12; Table 1). Healthy males had larger ICV than females (p=1×10^{-12}). Sulcal CSF volume was greater in men than in women (p=0.007), but the percentage of sulcal CSF-to-ICV was similar (p=0.26). Figure 1B shows the ability of DTI contrast to cluster tissue types based on mean diffusivity and FA [15, 25]. Brain parenchyma is clearly separable from the ventricular CSF (FA $<$ 0.20 & MD $>$ 0.0022 mm^2 sec^{-1}) in this two-dimensional quantitative space. Analysis of the water phantom data [28] acquired almost monthly over 4 years indicate stability over time (i.e. average FA $\pm$ S.D. = 0.015 $\pm$ 0.002; FA temporal correlation significance p=0.3; average MD $\pm$ S.D. = (1.88 $\pm$ 0.16) x10^{-3} mm^2 sec^{-1}; MD temporal correlation significance p=0.2, and a relative mean diffusivity coefficient of variation ~ (0.45 $\pm$ 0.06) %.

3.1 Comparison of DTI-based LV Segmentation with Validated FreeSurfer

Figure 2 Illustrates the coregistration T1w and DTI data to estimate the spatial overlap of DTI-based and T1w LV segmentations on one subject at one axial section. The average spatial overlap on the entire 105 subjects as measured by the Dice index is ~ (79.3 ± 3.9) % with range = [75.6 – 86.4] %, and median = 80.3 %. The Dice index was comparable between men and women (p=0.44). As illustrated in Figure 2 this value is slightly affected by the fidelity of the DTI-based mask interpolation which is expected to affect the surface boundaries of the LV.

3.2 LV Diffusivity Spatial Distribution

Figure 3 illustrates the spatial distribution of the lateral ventricular DTI metrics and shows (A) a fusion map of FA with MD from one healthy subject and (B) all 49 males and (C) all 56 females spatially normalized. Figure 3D, and 3E, show the histogram distributions of FA, and MD, respectively, on all 105 healthy subjects as the original LV mask is eroded from level 0 (volume = 11.42 mL) to level 8 (volume = 0.48 mL; see Figure 3E). Note that the mean diffusivity of CSF bordering brain parenchyma is lower than the values corresponding to central CSF.

3.3 LV Volume and Corresponding Diffusivity Gender and Age Effects

A previous multi-center study reported insignificant gender-based differences in brain parenchyma volumes in healthy controls and noted that CSF volume may have different growth rates in men and women [31]. The LVV-to-ICV normalized volume percentage (LVVp=LVV/ICV *100%) exhibited different age and gender effects in other reports [4, 13, 14]. Therefore, we analyzed and compared data between women and men. Table 1 provides a summary of ICV, LVV, LVVp, and corresponding DTI metrics (i.e. fractional anisotropy and mean diffusivity) in healthy men, women and the entire cohort.

The LVV obtained from the DTI and FreeSurfer methods correlated strongly for both men and women with an intraclass correlation coefficient of 0.99 (Figure 4A). The group averaged values of LVVp showed no difference between men and women using either FreeSurfer or DTI methods (p>0.76). The LVVp dependence on age was statistically significant *only in males* (p=0.01) using both T1w-FreeSurfer (Fig. 4B) and the DTI-based methods (Fig. 4C). The mean diffusivity values of lateral ventricular CSF (Fig. 4D) were slightly greater in males than in females (~1.2%; p=0.03). Mean diffusivity decreased with age at a comparable rate in both males and females (r=−0.3; p=0.02).

4. Discussion

In this work we validated a DTI-based segmentation method for lateral ventricular CSF segmentation in a large cohort of healthy controls. Our median estimate of the spatial overlap or concordance between the DTI-based method and a gold standard based on T1w was Dice ~ 80% on a large cohort of healthy controls which is comparable to previously reported methods of ~ [70–85] % for LV segmentation using manual delineations vs. automated methods [8, 19]. A major advantage of using DTI is the ability to work in each subject's brain native space (see Fig. 1B) in which DTI data are used to estimate attributes

of both gray matter [16] and white matter for tractography applications [24]. Alternatives to the DTI-based approach for ventricular segmentation would have required the co-registration of the T1-weighted data to the DTI space [32] or the co-registration of the DTI data to T1-weighted space [18] as attempted here to test the spatial overlap between the DTI and T1w methods.

The DTI-based segmentation of CSF in combination with spatial normalization methods provided the LV volume and corresponding DTI metrics on a large cohort of healthy males and females. We compared the DTI-based LVV results with those obtained with FreeSurfer using T1w and found strong correlation confirming previous reports that compared manual with automated methods for LV segmentation [8, 9, 19, 20]. The DTI-based segmentation approach was used previously to obtain global whole brain WM, GM and CSF attributes across the human lifespan [2]. In this report, the DTI-based segmentation was further combined with spatial normalization methods in SPM to obtain regional tissue attributes as has been applied to gray matter [16]. The current work applied DTI-based CSF segmentation with to segment the LV and compared the results with those obtained with a widely-used and validated approach that uses high resolution T1-weighted data [19, 20, 31]. Our results on the LV CSF diffusivity and FA compare well with previous reports despite slight variations in acquisition parameters [25, 27]. For example, Sidaros et al. [27] reported $FA(LV) \sim 0.13 \pm 0.05$ on healthy adults while our average values were 0.091 ± 0.012 (see Table 1).

4.1 Comparison of Age-related LV Volumetry with Literature

An important finding in our work is that the LVVp increased with age only in males while there was significant decrease in LV mean diffusivity in both males and females. Our work confirms previous reports on LV enlargement with healthy aging using postmortem [33, 34] and MRI data [3, 5, 35, 36]. Our results confirm a few reports on significant gender-based differences in the LV volumetry [4, 13, 14, 37, 38].

4.2 Neurobiological Implications of LV Volumetry

While the reasons for gender-based differences in the LV enlargement with age in young and middle-aged healthy adults are currently not well-understood, one may speculate on the potential role of hormones in regulating CSF compartmental volumes in women [39]. The study by Grant et al. [39] showed that CSF volume increased in women with a normal menstrual cycle and not taking oral contraceptives. Other factors such as plasma sodium concentration or osmolality that affect water retention in the brain may also regulate CSF volume [7].

4.2 Biophysical Implications of LV Diffusivity

Contributors to measured CSF diffusivity excluding non-random motion effects may include a host of biophysical factors that alter CSF viscosity such as temperature [11, 12, 40] and protein content [41]. Moreover, MRI signal changes in CSF have been related to dissolved oxygen content in CSF [42] and have been shown to also alter with CO_2 content [43].

A recent study by Sakai et al. [44] used calibrated water self-diffusion coefficient vs. temperature measurements [11, 12, 45] and a method for outlier rejection [12] to infer brain temperature in healthy adults. Sakai et al. [44] reported a steady decrease in LV temperature with age in healthy adults after ruling out other potential confounders such as protein content. Our results of a steady decrease of LV diffusivity with age are consistent with the findings by Sakai et al. [44], but note that they did not report gender-based differences in both LV volumetry and diffusivity as we have demonstrated. A slight decrease in water molecular diffusivity in females compared to males may be related to the expected cooling effects of greater cerebral blood flow in females [46, 47]. A steady decrease of core brain temperature with age may be related to reduced demand for energy [48] along with reduced dissipative heat generation [49] subsequent to neuronal and axonal dysfunction with natural aging [3].

4.3 Implications of our LV Results to Future Study Experimental Design

Our results on the significant differences between males and females in age-related LV enlargement despite comparable group averages caution that simple group averages is not reliable to account for age-related variance in the data. The adoption of covariance-based methods to correct for age differences is not warranted either as the growth slopes of LVVp with age are different between males and females, hence gender-based analyses are more appropriate [50]. Our results on differences between males and females on ventricular diffusivity may have implications to studies of the interplay between regional brain temperature and cerebral blood flow [49] and models of partial volume averaging of CSF on cortical or deep tissue diffusivity [32, 51, 52].

4.4 Limitations

This study has several limitations as we aimed primarily at presenting and validating a DTI-based method for estimating LV volumetry and corresponding diffusivity. We did not collect information from young and older females on their menstruation cycle, oral contraceptives, and menopause. In addition, due to acquisition time considerations, we did not acquire pulse-gated DTI data on the same subjects to study the effect of CSF pulsatility on the estimated mean diffusivity. This Report presented a retrospective analysis of DTI data collected using a protocol optimized primarily for whole brain parenchyma quantification at b=1000 s mm^{-2} and using 3mm sections with DTI scan time kept under 7 minutes to accommodate a wide range of ages and patient populations that were scanned at our imaging center. For combined CSF and brain tissue quantification, a DTI protocol with multiple b-factors (i.e. 400, 800 s mm^{-2}) and thinner slices (i.e. 1.5 mm) would have provided additional data to optimize the protocol for CSF volume and DTI quantification and test potential partial volume [26, 32, 51] and SNR estimation biases [25, 28]. Despite these limitations, our results warrant that DTI acquisition and analysis methods adopted in this work are reliable and stand on an equal footing with T1w data for reliable LV volume estimation and quantification.

4.5 Conclusion

In summary, we have presented and validated a DTI-based approach to segment CSF compartments and have shown its utility to quantify lateral ventricular volumetry and

diffusivity. We have applied the method to demonstrate gender and age effects that may be explored as potential neuroimaging markers.

Acknowledgments

References

1. Johanson CE, Duncan JA 3rd, Klinge PM, Brinker T, Stopa EG, Silverberg GD. Multiplicity of cerebrospinal fluid functions: New challenges in health and disease. Cerebrospinal Fluid Res. 2008; 5:10. [PubMed: 18479516]

2. Hasan KM, Sankar A, Halphen C, Kramer LA, Brandt ME, Juranek J, Cirino PT, Fletcher JM, Papanicolaou AC, Ewing-Cobbs L. Development and organization of the human brain tissue compartments across the lifespan using diffusion tensor imaging. Neuroreport. 2007; 18:1735–1739. [PubMed: 17921878]

3. Walhovd KB, Westlye LT, Amlien I, Espeseth T, Reinvang I, Raz N, Agartz I, Salat DH, Greve DN, Fischl B, Dale AM, Fjell AM. Consistent neuroanatomical age-related volume differences across multiple samples. Neurobiol Aging. 2011; 32:916–932. [PubMed: 19570593]

4. Grant R, Condon B, Lawrence A, Hadley DM, Patterson J, Bone I, Teasdale GM. Human cranial CSF volumes measured by MRI: sex and age influences. Magn Reson Imaging. 1987; 5:465–468. [PubMed: 3431356]

5. Scahill RI, Frost C, Jenkins R, Whitwell JL, Rossor MN, Fox NC. A longitudinal study of brain volume changes in normal aging using serial registered magnetic resonance imaging. Arch Neurol. 2003; 60:989–994. [PubMed: 12873856]

6. Carmichael OT, Kuller LH, Lopez OL, Thompson PM, Dutton RA, Lu A, Lee SE, Lee JY, Aizenstein HJ, Meltzer CC, Liu Y, Toga AW, Becker JT. Cerebral ventricular changes associated with transitions between normal cognitive function, mild cognitive impairment, and dementia. Alzheimer Dis Assoc Disord. 2007; 21:14–24. [PubMed: 17334268]

7. Gunduz-Bruce H, Narr KL, Gueorguieva R, Toga AW, Szeszko PR, Ashtari M, Robinson DG, Sevy S, Kane JM, Bilder RM. CSF sub-compartments in relation to plasma osmolality in healthy controls and in patients with first episode schizophrenia. Psychiatry Res. 2007; 155:57–66. [PubMed: 17398079]

8. Kempton MJ, Underwood TS, Brunton S, Stylios F, Schmechtig A, Ettinger U, Smith MS, Lovestone S, Crum WR, Frangou S, Williams SC, Simmons A. A comprehensive testing protocol for MRI neuroanatomical segmentation techniques: Evaluation of a novel lateral ventricle segmentation method. NeuroImage. 2011; 58:1051–1059. [PubMed: 21835253]

9. Chou YY, Leporé N, Avedissian C, Madsen SK, Parikshak N, Hua X, Shaw LM, Trojanowski JQ, Weiner MW, Toga AW, Thompson PM. Alzheimer's Disease Neuroimaging Initiative. Mapping correlations between ventricular expansion and CSF amyloid and tau biomarkers in 240 subjects with Alzheimer's disease, mild cognitive impairment and elderly controls. NeuroImage. 2009; 46:394–410. [PubMed: 19236926]

10. Mathew SJ, Mao X, Keegan KA, Levine SM, Smith EL, Heier LA, Otcheretko V, Coplan JD, Shungu DC. Ventricular cerebrospinal fluid lactate is increased in chronic fatigue syndrome compared with generalized anxiety disorder: an in vivo 3.0 T (1)H MRS imaging study. NMR Biomed. 2009; 22:251–258. [PubMed: 18942064]

11. Tofts PS, Jackson JS, Tozer DJ, Cercignani M, Keir G, MacManus DG, Ridgway GR, Ridha BH, Schmierer K, Siddique D, Thornton JS, Wroe SJ, Fox NC. Imaging cadavers: cold FLAIR and noninvasive brain thermometry using CSF diffusion. Magn Reson Med. 2008; 59:190–5. [PubMed: 18058937]

12. Kozak LR, Bango M, Szabo M, Rudas G, Vidnyanszky Z, Nagy Z. Using diffusion MRI for measuring the temperature of cerebrospinal fluid within the lateral ventricles. Acta Paediatr. 2010; 99:237–43. [PubMed: 19845565]

13. Blatter DD, Bigler ED, Gale SD, Johnson SC, Anderson CV, Burnett BM, Parker N, Kurth S, Horn SD. Quantitative volumetric analysis of brain MR: normative database spanning 5 decades of life. AJNR Am J Neuroradiol. 1995; 16:241–51. [PubMed: 7726068]

14. Chung SC, Tack GR, Yi JH, Lee B, Choi MH, Lee BY, Lee SY. Effects of gender, age, and body parameters on the ventricular volume of Korean people. Neurosci Lett. 2006; 395:155–158. [PubMed: 16300889]

15. Hasan KM, Halphen C, Sankar A, Eluvathingal TJ, Kramer L, Stuebing KK, Fletcher JM, Ewing-Cobbs L. Diffusion tensor imaging-based tissue segmentation: validation and application to the developing child and adolescent brain. NeuroImage. 2007; 34:1497–1505. [PubMed: 17166746]

16. Hasan KM, Frye RE. Diffusion tensor-based regional gray matter tissue segmentation using the international consortium for brain mapping atlases. Hum Brain Mapp. 2011; 32:107–117. [PubMed: 20799340]

17. Hasan KM, Narayana PA. Computation of the fractional anisotropy and mean diffusivity maps without tensor decoding and diagonalization: theoretical analysis and validation. Magn Reson Med. 2003; 50:589–598. [PubMed: 12939767]

18. Walimuni IS, Hasan KM. Atlas-based investigation of human brain tissue microstructural spatial heterogeneity and interplay between transverse relaxation time and radial diffusivity. NeuroImage. 2011; 57:1402–1410. [PubMed: 21658457]

19. Fischl B, Salat DH, Busa E, Albert M, Dieterich M, Haselgrove C, van der Kouwe A, Killiany R, Kennedy D, Klaveness S, Montillo A, Makris N, Rosen B, Dale AM. Whole brain segmentation: automated labeling of neuroanatomical structures in the human brain. Neuron. 2002; 33:341–355. [PubMed: 11832223]

20. Jovicich J, Czanner S, Han X, Salat D, van der Kouwe A, Quinn B, Pacheco J, Albert M, Killiany R, Blacker D, Maguire P, Rosas D, Makris N, Gollub R, Dale A, Dickerson BC, Fischl B. MRI-derived measurements of human subcortical, ventricular and intracranial brain volumes: Reliability effects of scan sessions, acquisition sequences, data analyses, scanner upgrade, scanner vendors and field strengths. NeuroImage. 2009; 46:177–192. [PubMed: 19233293]

21. Hasan KM, Walimuni IS, Abid H, Hahn KR. A review of diffusion tensor magnetic resonance imaging computational methods and software tools. Comput Biol Med. 2011; 41:1062–1072. [PubMed: 21087766]

22. Ashburner J, Friston KJ. Unified segmentation. NeuroImage. 2005; 26:839–851. [PubMed: 15955494]

23. Tzourio-Mazoyer N, Landeau B, Papathanassiou D, Crivello F, Etard O, Delcroix N. Automated anatomical labelling of activations in spm using a macroscopic anatomical parcellation of the MNI MRI single subject brain. NeuroImage. 2002; 15:273–289. [PubMed: 11771995]

24. Mori S, Oishi K, Jiang H, Jiang L, Li X, Akhter K, Hua K, Faria AV, Mahmood A, Woods R, Toga AW, Pike GB, Neto PR, Evans A, Zhang J, Huang H, Miller MI, van Zijl P, Mazziotta J. Stereotaxic white matter atlas based on diffusion tensor imaging in an ICBM template. NeuroImage. 2008; 40:570–582. [PubMed: 18255316]

25. Pierpaoli C, Jezzard P, Basser PJ, Barnett A, Di Chiro G. Diffusion tensor MR imaging of the human brain. Radiology. 1996; 201:637–648. [PubMed: 8939209]

26. Pfefferbaum A, Sullivan EV. Increased brain white matter diffusivity in normal adult aging: relationship to anisotropy and partial voluming. Magn Reson Med. 2003; 49:953–961. [PubMed: 12704779]

27. Sidaros A, Engberg AW, Sidaros K, Liptrot MG, Herning M, Petersen P, Paulson OB, Jernigan TL, Rostrup E. Diffusion tensor imaging during recovery from severe traumatic brain injury and relation to clinical outcome: a longitudinal study. Brain. 2008; 131:559–572. [PubMed: 18083753]

28. Hasan KM. A framework for quality control and parameter optimization in diffusion tensor imaging: theoretical analysis and validation. Magn Reson Imaging. 2007; 25:1196–1202. [PubMed: 17442523]

29. Shrout PE, Fleiss JL. Intraclass correlations: uses in assessing rater reliability. Psychol Bull. 1979; 86:420–428. [PubMed: 18839484]

30. Zou KH, Tuncali K, Silverman SG. Correlation and simple linear regression. Radiology. 2003; 227:617–622. [PubMed: 12773666]

31. Fjell AM, Westlye LT, Amlien I, Espeseth T, Reinvang I, Raz N, Agartz I, Salat DH, Greve DN, Fischl B, Dale AM, Walhovd KB. Minute effects of sex on the aging brain: a multisample magnetic resonance imaging study of healthy aging and Alzheimer's disease. J Neurosci. 2009; 29:8774–8783. [PubMed: 19587284]

32. Jeon T, Mishra V, Uh J, Weiner M, Hatanpaa KJ, White CL 3rd, Zhao YD, Lu H, Diaz-Arrastia R, Huang H. Regional changes of cortical mean diffusivities with aging after correction of partial volume effects. NeuroImage. 2012; 62:1705–1716. [PubMed: 22683383]

33. Hubbard BM, Anderson JM. Age, senile dementia and ventricular enlargement. J Neurol Neurosurg Psychiatry. 1981; 44:631–635. [PubMed: 7288452]

34. Pakkenberg B, Gunderse HJ. Neocortical neuron number in humans: effect of sex and age. J Comp Neurol. 1997; 384:312–320. [PubMed: 9215725]

35. Goodro M, Sameti M, Patenaude B, Fein G. Age effect on subcortical structures in healthy adults. Psychiatry Res. 2012; 203:38–45. [PubMed: 22863654]

36. Long X, Liao W, Jiang C, Liang D, Qiu B, Zhang L. Healthy aging: an automatic analysis of global and regional morphological alterations of human brain. Acad Radiol. 2012; 19:785–793. [PubMed: 22503890]

37. Agartz I, Sääf J, Wahlund LO, Wetterberg L. Quantitative estimations of cerebrospinal fluid spaces and brain regions in healthy controls using computer-assisted tissue classification of magnetic resonance images: relation to age and sex. Magn Reson Imaging. 1992; 10:217–226. [PubMed: 1564991]

38. Matsumae M, Kikinis R, Mórocz IA, Lorenzo AV, Sándor T, Albert MS, Black PM, Jolesz FA. Age-related changes in intracranial compartment volumes in normal adults assessed by magnetic resonance imaging. J Neurosurg. 1996; 84:982–991. [PubMed: 8847593]

39. Grant R, Condon B, Lawrence A, Hadley DM, Patterson J, Bone I, Teasdale GM. Is cranial CSF volume under hormonal influence? An MR study. J Comput Assist Tomogr. 1988; 12:36–39. [PubMed: 3335669]

40. Cappelezzo M, Capellari CA, Pezzin SH, Coelho LA. Stokes-Einstein relation for pure simple fluids. J Chem Phys. 2007; 126:224516. [PubMed: 17581072]

41. Brydon HL, Hayward R, Harkness W, Bayston R. Physical properties of cerebrospinal fluid of relevance to shunt function. 1: The effect of protein upon CSF viscosity. Br J Neurosurg. 1995; 9:639–644. [PubMed: 8561936]

42. Zaharchuk G, Martin AJ, Rosenthal G, Manley GT, Dillon WP. Measurement of cerebrospinal fluid oxygen partial pressure in humans using MRI. Magn Reson Med. 2005; 54:113–121. [PubMed: 15968660]

43. Teasdale GM, Grant R, Condon B, Patterson J, Lawrence A, Hadley DM, Wyper D. Intracranial CSF volumes: natural variations and physiological changes measured by MRI. Acta Neurochir Suppl (Wien). 1988; 42:230–235. [PubMed: 3189015]

44. Sakai K, Yamada K, Mori S, Sugimoto N, Nishimura T. Age-dependent brain temperature decline assessed by diffusion-weighted imaging thermometry. NMR Biomed. 2011; 24:1063–1067. [PubMed: 21274962]

45. Mills R. Self-diffusion in normal and heavy-water in range 1–45 degrees. J Phys Chem. 1973; 77:685–688.

46. Liu Y, Zhu X, Feinberg D, Guenther M, Gregori J, Weiner MW, Schuff N. Arterial spin labeling MRI study of age and gender effects on brain perfusion hemodynamics. Magn Reson Med. 2012; 68:912–922. [PubMed: 22139957]

47. Gur RC, Mozley LH, Mozley PD, Resnick SM, Karp JS, Alavi A, Arnold SE, Gur RE. Sex differences in regional cerebral glucose metabolism during a resting state. Science. 1995; 267(5197):528–531. [PubMed: 7824953]

48. Kety SS. Human cerebral blood flow and oxygen consumption as related to aging. J Chronic Dis. 1956; 3:478–486. [PubMed: 13306754]

49. Yablonskiy DA, Ackerman JJ, Raichle ME. Coupling between changes in human brain temperature and oxidative metabolism during prolonged visual stimulation. Proc Natl Acad Sci U S A. 2000; 97:7603–7608. [PubMed: 10861022]

50. Pfefferbaum A, Rohlfing T, Rosenbloom MJ, Chu W, Colrain IM, Sullivan EV. Variation in longitudinal trajectories of regional brain volumes of healthy men and women (ages 10 to 85years) measured with atlas-based parcellation of MRI. NeuroImage. 2013; 65:176–193. [PubMed: 23063452]

51. Alexander AL, Hasan KM, Lazar M, Tsuruda JS, Parker DL. Analysis of partial volume effects in diffusion-tensor MRI. Magn Reson Med. 2001; 45:770–780. [PubMed: 11323803]

52. Latour LL, Warach S. Cerebral spinal fluid contamination of the measurement of the apparent diffusion coefficient of water in acute stroke. Magn Reson Med. 2002; 48:478–486. [PubMed: 12210912]
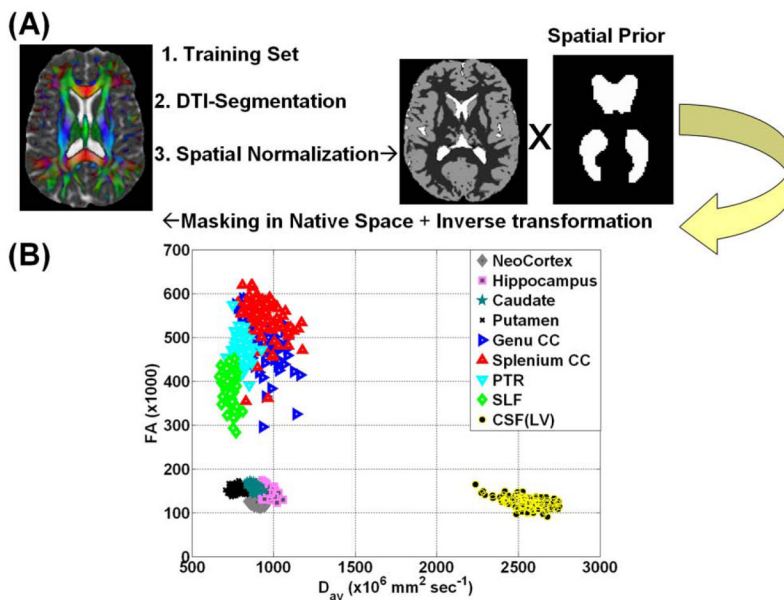
Figure 1.
(A) A flow chart of the main steps used in segmentaing the LV in native space using the DTI contrast, spatial normalization and LV template (B) A two-dimensional scatter plot of the MD vs. FA of several representative white matter, gray matter structures and lateral ventricular CSF. Note that MD(LV) ~ 2.5 * MD(parenchyma) enabling reliable CSF segmentation.
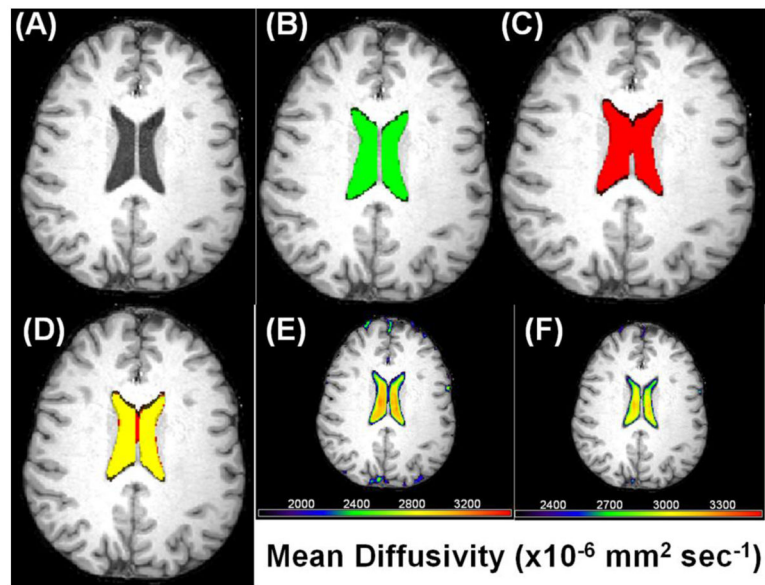
Figure 2.
Illustration of the coregistration and fusion of DTI and T1w volumes to estimate the spatial overlap on one subject at one axial section (A) T1w (B) The LV mask using T1w (green) (C) LV mask using DTI (red) (D) A fusion of the two masks (red and green gives yellow for the overlap; Dice index ~ 85% in this case) (E) A fusion of the mean diffusivity map and T1w to illustrate the effect of partial averaging of LV CSF with parenchyma which is reduced in (F) increasing the mean diffusivity threshold.
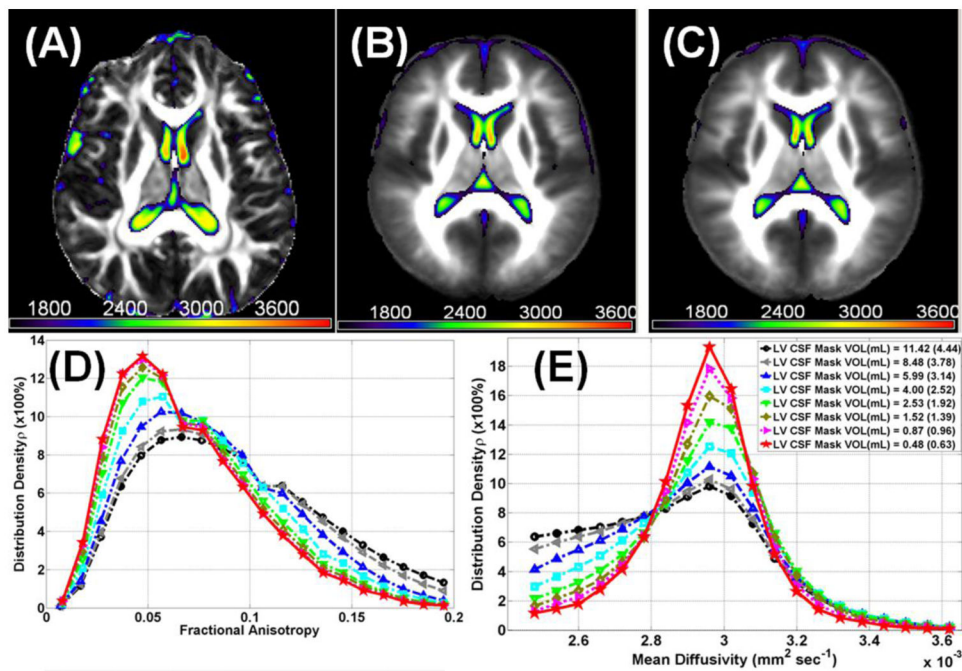
Figure 3.
Demonstration of quality assurance and analysis of spatial distribution of the lateral ventricular DTI metrics **(A)** a fusion map of fractional anisotropy from one healthy mean diffusivity and subject and **(B)** all 49 males, and **(C)** all 56 females spatially normalized using SPM in MNI space (see Methods). The color bar corresponds to mean diffusivity values ($\times 10^6 mm^2 sec^{-1}$). Histogram distributions of lateral ventricular **(D)** fractional anisotropy, **(E)** mean diffusivity of all 105 healthy subjects as the original LV mask is eroded from level 0 (avg. volume = 11.42 mL) to level 8 (avg. volume =0.48 mL). Note that the mean diffusivity of CSF bordering brain parenchyma is lower than the values corresponding to central CSF and LV mask erosion in each subject native space provided accurate estimation of DTI metrics.
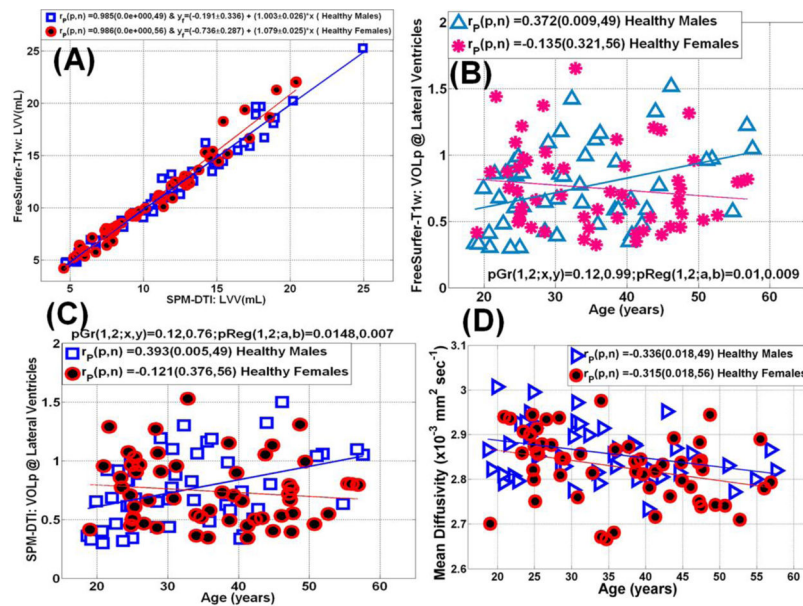
Figure 4.
(A) Scatter plot and linear regression of the lateral ventricular volume obtained using the DTI segmentation and FreeSurfer (see Table 1). **(B)** A scatter plot and regression analysis of the sensitivity of the normalized LV-to-intracranial volume percentage obtained using FreeSurfer to age in both men and women, note the significant increase in LV volume in men. **(C)** A scatter plot and regression analysis of the sensitivity of the normalized LV-to-intracranial volume percentage obtain using the DTI-based method to age in both men and women (compare the trends in men and women to those obtained using FreeSurfer Fig. 2C) **(D)** Scattter and regression analysis of lateral ventricular mean diffusivity in men and women.

Table 1

Demographics, MRI characteristics of healthy males and females.

	Entire Healthy Group (N=105)	Males (M=49)	Females (F=56)	p (M vs. F)
Age in years:				
Mean ± S. D.	34.8 ± 10.6	33.1 ± 10.5	36.3 ± 10.5	0.12
[Range]	[18.7 – 57.6]	[18.7 – 57.6]	[19 – 56.9]	
Median	33.7	30.7	35.8	
Intracranial Volume (mL) Mean ± S. D.	1529.4 ± 136.2	1620.6 ± 109.7	1449.6 ± 103.4	**1×10^{-12}**
Sulcal CSF Volume(mL)	119.8 ± 42.7	131.7 ± 45.9	109.4 ± 37	**0.007**
sCSFp (sCSFv/ICV*100%)	7.81 ± 2.57	8.11 ± 2.68	7.54 ± 2.47	0.26
LVV (mL)				
SPM-DTI	11.42 ± 4.44	12.21 ± 4.72	10.73 ± 4.11	0.09
FreeSurfer	11.40 ± 4.66	12.05 ± 4.80	10.84 ± 4.50	0.19
LVVp				
SPM-DTI	0.749 ± 0.292	0.759 ± 0.306	0.741 ± 0.282	0.76
FreeSurfer	0.748 ± 0.307	0.749 ± 0.312	0.748 ± 0.306	0.99
MD(LV)	2.844 ± 0.00071	2.862 ± 0.00062	2.828 ± 0.00075	**0.02**
FA(LV)	0.091 ± 0.012	0.089 ± 0.011	0.092 ± 0.012	0.22

Abbreviations

ICV = Intracranial volume (mL)

LVV= lateral ventricular volume (mL)

LVVp = Lateral ventricular volume to total intracranial volume percentage = LVV/ICV (×100%)

S.D. = standard deviation; M = males, F = females

FA = Fractional anisotropy

MD = Mean diffusivity ($mm^2\ sec^{-1}$).

sCSF = sulcal or non-ventricular CSF